Quaternary Science Reviews
June 2008, Volume 27, Issues 11-12, Pages 1107-1123
http://dx.doi.org/10.1016/j.quascirev.2008.02.009

Coastal dynamics under conditions of rapid sea-level rise: Late Pleistocene to Early Holocene evolution of barrier–lagoon systems on the northern Adriatic shelf (Italy)

Joep E.A. Storms[a, *], Gert Jan Weltje[a], Guido J. Terra[b], Antonio Cattaneo[c] and Fabio Trincardi[d]

[a] Faculty of Civil Engineering and Geosciences, Delft University of Technology, Section Applied Geology, PO Box 5028, NL-2600GA Delft, The Netherlands
[b] Physics Department, Royal Netherlands Institute for Sea Research (NIOZ), PO Box 59, NL-1790AB Den Burg, The Netherlands
[c] IFREMER-Centre de Brest, Département Géosciences Marines, BP 70, F-29280 Plouzané, France
[d] Istituto di Scienze Marine-ISMAR (CNR), Via Gobetti 101, I-40129 Bologna, Italy

*: Corresponding author : Storms J., email address : j.e.a.storms@tudelft.nl

Abstract:

This multidisciplinary case study of two preserved barrier systems combined the analysis of radiocarbon datings, grain-size distributions, high-resolution seismics, and shelf bathymetry with reconstructions of palaeo-environmental conditions (tides, waves, sea-level change) and forward modelling of barrier–lagoon systems, to provide an integrated view of the coastal transgressive evolution of a large sector of the northern Adriatic shelf between 15 and 8 ka BP. Palaeo-environmental reconstructions point to increased tidal amplitude, low-energy wave climate and high rates of sea-level rise (up to 60 mm/a) during the formation of the oldest preserved barrier system (not, vert, similar90 m water depth; 14.3 cal ka BP). A younger barrier system (42 m water depth; 10.5 cal ka BP) formed under conditions of lower tidal amplitude, higher wave energy and a lower rate of sea-level rise (10 mm/a).

Forward modelling suggests that the probability of barrier-island overstepping during transgression is inversely proportional to tidal amplitude, if all other factors are assumed equal. The oldest barrier–lagoon system developed under conditions of large tidal amplitude, which permitted rapid transgression. However, this system apparently failed to keep up with the anomalously high rate of sea-level rise resulting from melt-water pulse 1A. The youngest barrier system appears to have drowned in place due to antecedent topography. As the barrier system transgressed over an ancient Pleistocene alluvial plain, the rapid increase in backbarrier accommodation caused an abrupt disequilibrium between shoreface and backbarrier sedimentation, which led to barrier overstepping. Although BarSim modelling indicates that tidal deposition can reduce the probability of barrier overstepping, there are other driving mechanisms (in our case extremely rapid sea-level rise and antecedent topography), which are more determinative in explaining the transgressive coastal evolution of barrier–lagoon systems in the northern Adriatic Sea.

Grain-size analysis of shoreface deposits sampled above the transgressive ravinement surface across the northern Adriatic shelf indicate a distinct relation between the sediment grain size and the rate of sea-level rise during deposition, which implies that progressive sorting must have been highly effective.

Keywords: sea-level rise, transgression, barrier-lagoon system, tidal amplification, forward modelling, progressive sorting.

1. Introduction

Late Quaternary clastic transgressive coasts often consist of typical barrier-lagoon systems that continuously migrate landwards as sea level rises (e.g., Swift, 1968; Belknap and Kraft, 1981; Nummedal and Swift, 1987). This type of transgression (continuous retreat; Swift et al., 1991) is generally accepted as the dominant type of retreat. However, Rampino and Sanders (1980, 1982, 1983) describe a more controversial discontinuous retreat model (see discussions by Swift and Moslow, 1982; Leatherman, 1983) which assumes that a barrier system may be overstepped if the rate of sea-level rise is fast enough to drown the complete barrier in place while the shoreline steps landward. Rampino and Sanders (1980) lend credence to their theory by identification of offshore lagoonal deposits and bars, but they were not the first to describe the overstepping theory. Curray (1964) and Swift (1968) described a mechanism whereby barriers tend to grow upward during transgression until their enlarged lagoons trap so much sediment that the barrier is overstepped. Shoreface reworking generally destroys all evidence of the mode of retreat, thus leaving little evidence for the discontinuous retreat model. However, Forbes et al. (1991) illustrated barrier overstep for gravel barriers while Gardner et al., 2005 and Gardner et al., 2007 show preserved barriers at the outer shelf from high-resolution multibeam surveys. Here we present a new dataset based on a palaeo-environmental reconstruction for the Northern Adriatic Shelf which may shed a new light on the discussion of barrier overstep versus continuous retreat.

The Adriatic Sea is a low-gradient shelf sea in which sediment accumulated during the last transgression to form a continuous record in the centre of the basin and a set of discrete sediment bodies on the shelf. The latter are represented by two isolated areas comprising preserved barrier-lagoon deposits, which originated during the Late Pleistocene and Holocene sea-level rise (Trincardi et al., 1994; Correggiari et al., 1996a; Cattaneo and Trincardi, 1999). The barrier-lagoon deposits occur at different present-day water depths. They are separated from one another by a distance of more than 150 km and by a time interval of nearly 5000 years. Each of the sediment bodies represents a snapshot of coastal evolution during the post-glacial sea-level rise which started around 18 ka BP (Fairbanks, 1989; Bard et al., 1996).

A comparative analysis of the two barrier-lagoon systems was carried out by means of a multidisciplinary approach in which analysis of various types of data (shallow seismics, core descriptions, grain-size distributions and radiocarbon dating) was combined with process-response simulation of barrier-lagoon systems under conditions of rapid sea-level rise. Forward modelling is based on an adaptation of BarSim (Storms, 2003). The inferred rates of post-glacial sea-level rise under which the two systems evolved far exceeded any observed in historical times, which indicates that these isolated barrier-lagoon systems cannot be directly compared to modern coastal environments. However, understanding their dynamics is essential since they provide well-documented ancient analogues to possible future scenarios of coastal evolution under conditions of accelerated sea-level rise. In the Adriatic region, the isolated sediment bodies are also of commercial interest, because they represent exploitable resources of clean sand.

2. Geological setting of the Northern Adriatic shelf

The Adriatic Sea is a mid-latitude semi-enclosed rectangular basin bordered to the Southwest by the Apennines, to the North by the Alps and to the Northeast by the Dinaric Alpes. The Adriatic Sea is on average 200 km wide and approximately 800 km long (Fig. 1). It may be subdivided into three bathymetrically distinct regions. The northern region consists of a 300 km long south-sloping low-gradient continental shelf bordered by the 120-m isobath. The adjacent middle region comprises several slope basins, including the Meso-Adriatic Depression (=MAD), which has a maximum water depth of 260 m. The southern region, which is connected to the Mediterranean Sea by the narrow Strait of Otranto, is much deeper (up to 1200 m). The shelf North of the Gargano Promontory is a modern foreland basin related to the Cenozoic emplacement of the Apenninic chain (Argnani et al., 1991). The depth of the base of the Pliocene increases landward from 1 to 3 km, which indicates high rates of tectonically induced flexural subsidence north of the Gargano Promontory during the Quaternary (Pieri and Groppi, 1981; Waschbusch and Royden, 1992; Ridente and Trincardi, 2002). Subsidence patterns in the Northern Adriatic basin over the last 15 ka are poorly constrained (Pirazzoli, 2005).

The Northern Adriatic shelf is characterized by a very low gradient in its northern and central parts, and a high gradient in the southwest. During the Last Glacial Maximum (=LGM), an approximately 300 km wide stretch of the Northern Adriatic shelf was subaerially exposed. The drainage network on this large alluvial plain likely comprised a “Mega Po” trunk river, with the Alpine and Apenninic rivers as tributaries. The system terminated in a lowstand delta located at the northern edge of the MAD (Trincardi and Correggiari, 2000; Ridente and Trincardi, 2006). High-resolution seismic surveys have indicated the presence of isolated incised valleys at various locations on the shelf, and systematic mapping of the Late-Pleistocene palaeo-Po valley is being conducted within the national (Italian) project Cartografia Marina (Trincardi and Argnani, 2001; Trincardi et al., 2004). Preliminary work shows that incised valleys and channels are not continuous but appear locally deepened or completely erased in other areas and depth intervals (Trincardi et al., 1994). Prior to 9 ka BP, sedimentation in the coastal plain (the present onshore) was restricted to the incised valley of the Po and its tributaries, while pedogenesis took place on the interfluves (Amorosi et al., 2003). Sediment supply by the Po River and various smaller Apenninic and Alpine rivers has been significant during the Late Quaternary sea-level rise (Kettner and Syvitski, in press), whereas sediment input from the Dinarides has been negligible due to their carbonatic lithology and the presence of nearshore structural basins acting as sediment traps. The majority of the fluvial sediment, which was fine grained, has been trapped in an elongated mud wedge along the high-gradient south-western shelf (Fig. 1; Cattaneo et al., 2003) due to the presence of an anti-clockwise circulation pattern. This coast-hugging oceanic current reflects a combination of wind forcing by Bora and Sirocco and thermohaline circulation (Decouttere et al., 1998). It is inferred to have been active since the late Pleistocene, ~15 ka BP (Trincardi et al., 1994; Correggiari et al., 1996b; Cattaneo and Trincardi, 1999). Consequently, the northern part of the shelf acted as a bypass zone and has been starved of sediment during the past 15 ka.

The late-Quaternary transgressive deposits of the northern shelf consists of two main isolated shallow-marine sediment bodies located at approximately 90 m and 42 m below present sea level (Fig. 2). These isolated sediment bodies are interpreted as preserved barrier-lagoon complexes. The average rate of transgression between the 120 m and 26 m isobath, corresponding to the inferred coastline positions at 19 ka BP

(LGM) and 9 ka BP, respectively, was 28 m/a. The rate of transgression was even higher during the two melt-water pulses (Fairbanks, 1989; Clark et al., 2002; Liu and Milliman, 2004). Such rates of transgression far exceed any observed during historical times, which indicates that these ancient barrier-lagoon complexes cannot be directly compared to modern depositional systems.

3. Palaeoceanographic conditions

3.1. Sea-level history

Although the Mediterranean and Adriatic seas are semi-enclosed basins, they remained connected to the Atlantic Ocean during the LGM. This implies that the eustatic sea-level curve should be applicable to the Adriatic Sea. Coastal dynamics are highly sensitive to changes in the rate of sea-level rise, especially on low-gradient shelves such as the Northern Adriatic. It is therefore important to constrain the rates of sea-level rise during the time interval corresponding to the formation of the barrier-lagoon systems as accurately as possible. Liu and Milliman (2004) presented new data to refine the depth ranges and timing of melt water pulses MWP-1A (96 to 76 m below present sea level; 14.3 to14.0 ka cal BP) and MWP-1B (58 to 45 m below present sea level; 11.5 to 11.2 ka cal BP). As the time interval of interest to this study is between 15 ka BP and 8 ka BP, we used the Liu and Milliman (2004) curve, and extended it with data from Fleming et al. (1998) for the interval between 10 ka BP and 8 ka BP (Fig. 3).

Reconstruction of a relative sea-level curve applicable to the Northern Adriatic requires that the eustatic signal be combined with information on local subsidence due to tectonics, sediment loading and compaction. Although such information is available for some areas of the northern Adriatic, for instance the modern Po plain, where subsidence rates are locally up to 2 mm/a (Brunetti et al., 1998; Carminati and Di Donato, 1999), there is no comprehensive analysis of vertical movements in the offshore (Pirazzoli, 2005). In the Venice area, the average subsidence rate over the past 400 ka is estimated to be 0.36 mm/a, based on data from a 950 m deep core (Kent et al., 2002). About 60 km south of the present Po delta, the Eemian shoreline (~120 ka BP) is identified at 120 m depth below the modern coastal plain of Ravenna

(Amorosi et al., 1999). This would suggest an average combined subsidence and compaction rate of about 1 mm/a. In the north-eastern part of the Adriatic, however, relative sea level appears to have been stable during the late Holocene (Pirazzoli, 2005). Subsidence rates further to the south are poorly known, but the presence of a palaeo-shoreline (lowstand delta) at ~120 m water depth (Trincardi and Correggiari, 2000) indicates that the local sea-level lowstand closely matches the inferred global (eustatic) lowstand of ~125 m below present sea level (Fleming et al., 1998), which would imply that net subsidence in the area North of the MAD has been negligible. In the absence of detailed information on subsidence patterns of the northern Adriatic shelf, we decided to adopt the uncorrected eustatic sea-level curve as a proxy of relative sea-level history. The corresponding transgression scenario was compared to an extensive set of radiocarbon datings of backbarrier peat (Correggiari et al., 1996a; Trincardi and Argnani, 2001, ISMAR, unpublished data) to examine the validity of this assumption (see below).

3.2. Palaeo-tidal regime

The northern Adriatic is presently characterized by a micro-tidal regime. The lunar semidiurnal M2 tidal amplitude increases from south to North due to a decrease in water depth. Offshore of Venice, the M2 tidal range is about 0.2 m. Locally, tidal ranges may be up to 1 m due to resonance effects in embayments, for instance near Trieste (Bondesan et al., 1995). Although several models were developed to simulate present-day tidal dynamics in the Adriatic (Malačič et al., 2000; Cushman-Roisin and Naimie, 2002) little is known about palaeo-tidal regimes. Of particular interest in the context of this study is whether the elongate land-locked Adriatic basin may have exhibited transient tidal-resonance effects during the post-glacial sea-level rise, which caused the basin to widen and changed its shape (Cattaneo and Trincardi, 1999). If so, traces of this response may be preserved in the sediments.

To test this hypothesis, we developed a simple idealized 1-D model for tidal motion, in which the Adriatic Sea was assumed an elongated box and cross-sectional variations in water depth were neglected. The present bathymetry of the northern shelf was used to derive an approximation of the initial (lowstand) topography in the form of a series of line segments (Fig. 4). This profile represents the water depth along the

axis of the basin. In order to properly approximate the basin in 1-D, a transversally averaged effective depth has been used, biased towards the (deeper) parts with higher velocities. The effective water depth *D* was defined by multiplication of the maximum depth along the central axis by 0.85. In the analytical model, the influence of the Earth's rotation is not taken into account and friction is neglected, which implies that no damping occurs. Because the amplitude of the tidal motion is small and the wavelength is large relative to *D*, the 1-D linearized shallow-water equations have been used:

$$\frac{\partial \zeta}{\partial t} + \frac{\partial}{\partial x}\left[D(x)u\right] = 0$$

$$\frac{\partial u}{\partial t} = -g\frac{\partial \zeta}{\partial x},$$

where:

$\zeta = \zeta_e(t)$ at the open (southern) boundary

$\zeta, u < \infty$ at the closed (northern) boundary

In the above equations, *D(x)* is the longitudinal depth profile in km and *g* is the gravitational acceleration in m^2/s. The *x*-coordinate runs northward along the central axis of the basin. The variable ζ denotes the water-level elevation (m) relative to the water-level elevation at rest, and *u* is the averaged velocity (m/s) in northward direction. Water-level elevation is prescribed to be $\zeta_e = \alpha_e \cos(\omega t)$ at the open (southern) boundary. The angular forcing frequency for the M2 semidiurnal tidal component is $\omega_{M2} = 2\pi / 44700 = 1.4 \cdot 10^{-4}$ rad/s and the present tidal amplitude at the connection between the Adriatic and the Mediterranean Sea is $\omega_{e,M2} = 0.08$ m. For the K1 diurnal tidal component these numbers are $\omega_{K1} = 2\pi / 86162 = 7.3 \cdot 10^{-4}$ rad/s and $\omega_{e,K1} = 0.04$ m, respectively. Palaeo-tidal responses at various sea levels have been computed for the same forcing conditions.

The tidal amplitudes are shown as a function of coastline position *x* for different Late Quaternary sea levels (Fig. 5). The length of the basin increased over time as sea level rose. The results for the present-day situation correspond well with the observations

reported by Polli (1960). For the K1 tidal component, the fit depends significantly on the depth-correction factor of 0.85, whereas the results for the M2 tidal component are relatively insensitive to this correction. Modelling results show that amplification of the M2 tidal component was most pronounced at x = 317 km, where at present the water depth is 75 m along the central axis. Because damping due to friction for example is not included in this simple model, the resonance leads to a singular response in that situation. In reality, radiation of energy into the Mediterranean Sea is expected to keep amplification within reasonable bounds. On the other hand, amplification of the K1 tidal component increases with rising sea level. Although the exact tidal ranges are speculative, due to limitations of the model and uncertainties in boundary conditions, the modelling results clearly suggest that the older of the two barrier-lagoon systems was tidally influenced. Hence, cores and seismic profiles of backbarrier deposits may show remnants of tidal flats and channels. The tidal range decreased rapidly during subsequent sea-level rise, which indicates that tidally influenced transgressive deposits are much less likely to occur at shallower depths.

3.3. Palaeo-wave climate

Two major storm fields force the wave field in the Adriatic: the Bora and the Sirocco. During Bora storms, the wind is blowing from the northeast whereas Sirocco storms are characterized by steady winds from the southeast (Decouttere et al., 1998). The shape of the wave spectrum depends on the fetch length and the duration of the storm. Sirocco winds typically blow along the axis of the Adriatic Sea for several days and cause high swell waves in the northern part of the basin. In addition, the surge that accompanies a storm with a ten-year recurrence interval elevates average sea level in the Northern Adriatic by more than 1 m (Yu et al., 1998). The waves generated during a Sirocco event (large fetch and associated surge) are expected to be the most effective for reworking of shallow-marine sediments.

As the shallow northern Adriatic shelf flooded during the Late-Quaternary sea-level rise, its area increased sevenfold and the fetch increased significantly. The fetch increase is especially relevant for Sirocco events, during which the wind direction is parallel to the elongation of the basin. Significant wave height and period

corresponding to a given fetch have been calculated using equations for fetch-limited conditions (Corps of Engineers, 1984):

$$H_s = 5.112 \cdot 10^{-4} U_a \sqrt{f}$$

$$T_m = 6.238 \cdot 10^{-2} \sqrt[3]{U_a f}$$

where H_s is the significant wave height (m), f is the fetch (m) and T_m is the period (s) of the peak of the wave spectrum. U_a is adjusted wind speed (m/s), given by:

$$U_a = 0.71 U^{1.23},$$

where U is the wind speed at 10 m above the water surface. The direction of wave propagation is set equal to the wind direction (cf. Slingerland and Keen, 1999). In this case, wind direction is 300^{o}, which would represent a Sirocco event.

Based on the calculations, fetch increase between the LGM and present caused an increase of significant wave height and period by 20% and 15%, respectively. As the northern Adriatic shelf has a relatively uniform slope, wave propagation during the late Quaternary is unlikely to have changed much since the LGM. However, possible changes in wind regime due to late Pleistocene climate changes are not included in these equations.

3.4. Palaeo-circulation pattern

The present-day surface circulation pattern of the northern Adriatic Sea consists of a large-scale counter clockwise baroclinic geostrophic structure with cyclonic gyres of thermohaline origin (Malanotte-Rizzoli and Bergamasco, 1983; Orlic et al., 1992; Artegiani et al, 1997). As a result of this counter clockwise circulation, a fine-grained sediment wedge (Fig. 1) is formed that consists of Po and the Apennine derived sediments that are dispersed southward and deposited in a narrow band along the Italian coast down to the Gulf of Manfredonia, in the area south of the Gargano promontory (Cattaneo et al., 2003). Analysis of high-resolution seismic data combined with radiocarbon datings from numerous cores indicate that the

transgressive portion of the sediment wedge is 40 to 50 km wide and up to 25 m thick. The transgressive deposits have been subdivided into three intervals of which the lowest (pre 15 ka BP) shows a patchy distribution of sediment depocenters, whereas the middle and upper units display a dominant alongshore trend similar to the modern sea-level highstand deposits (Cattaneo and Trincardi, 1999; Cattaneo et al., 2003). The architecture of the middle unit (deposited between 14.8 and 11.3 cal ka BP) reflects a transitional period in which the modern oceanographic circulation pattern was established. Hence, it appears from the stratigraphic data that the counter clockwise current was initiated ~15 ka BP, most likely as a result of the increase in basin size due to sea-level rise (Cattaneo and Trincardi, 1999).

3.5. Palaeo-environmental synthesis

A summary of the reconstruction of palaeo tides, wave climate, and rate of sea-level change is given in Figure 5a-c, which shows the various controlling factors as function of coastline position along a profile of the Northern Adriatic shelf from the MAD to Venice. The tidal amplitude derived from the analytical model reached a maximum during the early phase of transgression, when the coastline was located close to the edge of the MAD. The amplitude decreased gradually until it reached its present value at around 11 ka BP. The wave climate gradually changed as sea level rose. Rates of sea-level rise varied greatly, with two distinct peaks corresponding to melt-water pulses 1A and 1B (Fairbanks, 1989).

The eustatic sea-level curve (Fig. 3) was combined with the present-day bathymetry of the Northern Adriatic shelf along the profile (Fig. 5d) to reconstruct palaeo-coastline positions during transgression (Fig. 5e). Coastline position has been plotted together with the available radiocarbon dates of backbarrier deposits at the appropriate water depths. All radiocarbon datings cluster about the curve of palaeo-shoreline position. Modest deviations from the profile can be observed, which reflect uncertainties in palaeo-water depths of the samples from which the radiocarbon datings were obtained, in conjunction with uncertainties in radiocarbon ages, and local topographic variability, as not all samples are located on the profile (Fig. 2). The data appear to be fully consistent with the reconstructed shoreline evolution, which justifies our assumption that net subsidence along the profile can be considered negligible (provided the sea-level curve is correct). Although the melt-water pulses

388 only represent 3% of the time span for the Late-Quaternary sea level rise, their effect
389 is very significant as an estimated 36% of the northern Adriatic shelf will be affected
390 by these extremely rapid sea-level rises, owing to its low gradient (Fig. 5d).
391 The radiocarbon datings show that both studied isolated sediment bodies were
392 deposited while the oceanic counter clockwise circulation was already active. This
393 implies that during formation of the barrier-lagoon systems, most of the suspended
394 fluvial sediment supplied to the northern Adriatic coastline was being removed by
395 longshore currents to be redeposited at the south-western part of the inner shelf, with
396 the possible exception of the coarsest fraction, which would have remained behind as
397 a lag deposit.
398
399 **4. Sedimentological interpretation**
400
401 *4.1. Site A: deep barrier-lagoon system*
402
403 The shelf of the Northern Adriatic Sea between 100 and 80 m water depth is
404 characterized by a relatively high gradient and is dissected by meandering channels
405 (with lateral accretion surfaces), which are up to 20 km long and between 4 and 15 m
406 deep. The orientation of the channels is predominantly North-South. Shallow seismic
407 profiles (Cattaneo et al., 2001) show a laterally persistent peat layer that rests
408 conformably on the pre-transgressive deposits (Fig. 6). Some channels incise below
409 the peat layer (seismic profile II), whereas the bases of other channels coincide with
410 the peat layer (seismic profile I). Not all channels can be clearly tied to the relative
411 sea-level curve. Lateral-migration features, which are typical for tidal channels (see
412 for example seismic profile II), are not present in channels assumed to have originated
413 during a phase of incision associated with sea-level fall or lowstand conditions
414 (Trincardi et al., 1996). The seismic profiles also suggest that most of the channels are
415 not filled with sediment. An exception to this is a narrow (<500 m) incised
416 distributary channel of more than 15 m deep that is completely filled transgressive
417 deposits and which presently has no morphological expression (seismic profile IV).
418
419 The heterolithic infilling of the channel (Fig. 6; seismic profile IV) suggests that tidal
420 deposition may have played an important role during this phase of the transgression.
421 The tidal amplification inferred from modelling for this time interval (Fig. 5a) would

provide a potential scenario for an estuarine infill of this distributary channel. As sea level rose at a rate of more than 60 mm/a (Fig. 3 and Fig. 5), the distributary channel became an estuary and was filled with centimetre to millimetre-scale alternating silt and clay deposits from both marine and fluvial in origin. It is uncertain whether this channel was a distributary of the palaeo-Po or of a local river or possibly even a tidal channel. In the latter case there would have been no local fluvial sediment source to fill the channel and all the sediment must have been marine in origin. Seismic profile IV shows that the top of the channel infill is formed by a wave-ravinement surface (Fig. 6).

A thin peat layer on top of older, pre-transgressive sands forms the base of the backbarrier deposits. Its presence demonstrates that some backbarrier areas were sheltered from sediment input (Fig. 6**,** seismic profile II). The peat layer is covered by a 1 to 3 m thick coarsening-upward sequence characteristically associated with a transgressive backbarrier setting, suggesting that barrier islands were present during this phase of rapid sea-level rise. The inferred age of the peat layer in core AN97-31 (14.3 ka BP; Cattaneo et al., 2001; ISMAR, unpublished data) matches the reconstructed shoreline position at that time (Fig. 5). Two intervals consisting of lag deposits with an erosional base overly the backbarrier deposits. The mollusc assemblage on top of the lower erosion surface (Fig. 6; core AN97-31) is characterized by shallow-marine species, intermixed with some brackish and open-marine species (Cattaneo et al., 2001). The mollusc assemblage directly above the upper erosion surface comprises predominantly open-marine species. The presence of two superimposed erosion surfaces with shell lags of different palaeo-environmental significance suggests that the first is associated with incision by a tidal channel (i.e., a tidal ravinement surface). The second surface most likely represents a wave-ravinement surface as it separates shoreface sediments from backbarrier deposits (Cattaneo et al., 2001).

4.2. Site B: shallow barrier-lagoon system

A narrow elongated sand ridge at the 42-m isobath southeast of the modern Po delta can be traced for about 50 km along the palaeo-coast line (Fig. 2). Radiocarbon dating of a peat layer at the base of the sand ridge indicates an age of 10.5 ka BP

(Correggiari et al., 1996a) which agrees with the reconstructed coastline position (Fig. 5) . The morphological expression of the sand ridge strongly suggests that it is a drowned barrier island (Fig. 2). Sediment cores (Fig. 8) from the sand ridge show a coarsening-upward trend indicative of a barrier environment. Section V (Fig. 8) shows that the sand ridge dips slightly towards the south. Overall the ridges are between 2 and 3 meter thick. Two ravinement surfaces are recognised in the cores (Fig. 8). The upper ravinement surface (Rs) originates from wave reworking during transgression. The lower ravinement surface (tRs) most likely is caused by migrating tidal channels (Cattaneo and Steel, 2003). Morphologically, the drowned barrier-lagoon system shows similarities to the modern Venice lagoon with its narrow barrier islands and extensive backbarrier area. There is no evidence of a preserved tidal delta. Petrographic composition of the barrier sands indicates a Po-type source (Colantoni et al., 1990).

The overstepped barrier chain rests on a 25 km wide sub-horizontal platform. Seismic profiles (IDROSER, 1985, 1990) show that small channels filled with sediments of pre-transgressive age dominate the platform subsurface (Fig. 9). The abundant channel fills, 2 to 5 m deep and 100 to 300 m wide, are all present at the same stratigraphic level. Lateral channel migration is indicated by steeply dipping reflectors (both East and Westward), which represent point bars that are up to 300 m wide (Fig. 9). Locally, channel density is up to four channels per kilometre. The seismic data suggest that the platform may have originated as part of a low-gradient Pleistocene alluvial (braid) plain, but no core data are available to confirm this. The platform is bounded to the East by a steep, 5 m high escarpment that resembles the confinement of an older river terrace.

5. Grain-size analysis

5.1. Data and results

Seven cores (three from the deep barrier-lagoon system at Site A, three from the shallow system at Site B, and one from relict transgressive deposits in 24 m water depth (Correggiari et al., 1996a) were sampled for grain-size analysis (Fig. 10). All grain-size measurements were made with a laser-diffraction spectrophotometer

(Konert and Vandenberghe 1997). All cores show typical transgressive backbarrier sequences overlying pre-transgressive sediments. The pre-transgressive sediments are conformably overlain by a ~30 cm thick bed comprised of mud, organic-rich mud and peat (Fig. 10). This bed is followed by an upward-coarsening backbarrier sequence of variable thickness, which is bounded at the top by an erosional surface. This erosion surface represents the wave-ravinement surface.

The grain-size distributions of the backbarrier deposits below the wave-ravinement surface may be interpreted as mixtures of distinct end-member grain-size populations (Fig. 10), which appear to be fixed (cf. Weltje and Prins, 2003). Within each core, the relative abundances of these grain-size populations define overall coarsening-upward trends. These trends reflect the change from a distal to a more proximal backbarrier depositional environment which consistent with a transgressive barrier which in our case is evolves overstepped.

According to Friedman (1961) characteristics of the grain size distribution (c.f. mean grain size and skewness) can be used to identify sediments that have been transported under different energy regimes and transport conditions. Figure 11 shows cross-plots of skewness and mean grain size for three different facies (sandy shoreface deposits, silty-sandy backbarrier deposits and clayey backbarrier deposits). The cross plot for the clayey backbarrier deposits (Fig. 11A) appears to be uncorrelated, which is not surprising as these deposits result from suspension fallout in a relatively quiet environment. The cross plot of the silty to sandy backbarrier deposits (Fig. 11B) shows a clear relation between mean grain size and skewness. Inspection of the grain-size distributions (Fig. 10) reveals that this correlation arises from the mixing of silt and very-fine sand sized populations. This mixing pattern is inferred to reflect several factors: (1) distance from the barrier island, which acted as the local sand source; (2) variability of energy conditions, i.e. fair weather vs. storms (and associated washover deposits), to which the backbarrier is especially sensitive; (3) relative importance of tidal deposition. Samples from the sandy shoreface above the transgressive ravinement surface (Fig. 11C) display similar phenomena.

Overall, the sandy backbarrier and shoreface samples (Fig. 11B and C) show a relation between mean grain size and water depth, where the fine grained samples

524 come from the deep water cores while the coarse samples are retrieved from the
525 shallow water cores. This implies that shallow-water shoreface sands are on average
526 coarser-grained than shoreface sands from deeper water (with the exception of
527 samples from core AR 00-45).
528
529 *5.2. Interpretation*
530
531 Our palaeo-environmental reconstruction indicates that the barrier-lagoon systems
532 developed when the counter-clockwise circulation pattern was already well
533 established (Trincardi et al., 1996). This implies that the suspended sediment load
534 from the Po (the dominant sediment source) was effectively transported along the east
535 coast of the Adriatic Sea where it is deposited in the transgressive sediment wedge
536 (Fig. 1). It is uncertain how much sand was left behind near the river mouth which
537 would have been a potential sediment source for the barriers. Local transport
538 pathways for the river sand by longshore currents may different from the prevailing
539 oceanic currents. Furthermore, the position of the Po during the Late Quaternary is
540 still poorly known. It is uncertain whether the Po was located to the east or to the west
541 of the barrier-lagoon system. In view of these uncertainties, it is not possible to
542 reconstruct the sediment supply of the barrier-lagoon system from fluvial sources.
543 Nevertheless, cores and seismic profiles suggest that the amount of sand on the
544 Adriatic shelf is low. Between the preserved two barrier-lagoon system, the pre-
545 transgressive Pleistocene sediments not covered by transgressive sands which implies
546 that the supply of sand must have been limited or local. The shoreface sand source
547 therefore must be a mixture of fluvial (Po) origin and reworked Pleistocene substrate
548 sediments. If we consider the grain size of the Pleistocene substrate to have been
549 spatially homogeneous and the rate of sediment supply by longshore drift limited, we
550 may assume that the grain-size of the shoreface primarily reflects progressive sorting
551 by continuous reworking (Swift et al., 1991). Such conditions cause a progressive
552 coarsening of the shoreface, which represents a lag deposit, because fine-grained
553 sediment is moved to the backbarrier area and carried offshore. The latter will be
554 transported along with the prevailing oceanic currents to the transgressive sediment
555 wedge. This suggests that the amount of time available for reworking may be
556 mirrored in the grain size of the shoreface deposits (Guillén and Hoekstra,1996). Yet,
557 this is largely dependent on both the grain-size and amount of sediment supplied in

time by both fluvial and substrate sources. Figures 12A and B show that there is no relation between the rate of sea level rise, which is a function of reworking time, and the grain size of the backbarrier deposits. Nor is there a relation between tidal amplitude, wave climate and the grain size of the backbarrier deposits (not shown here). This suggests that tidal deposition and washover are not significantly influenced by the rate of sea level rise. However, Figure 12C shows an overall negative correlation between the grain size of the shoreface sands and the rate of sea-level rise.

6. Effects of tides and waves

6.1. BarSim model

An adapted version of the numerical model BarSim (Storms et al., 2002; Storms, 2003; Storms and Swift, 2003) was used to evaluate the effects of tidal and washover on coastal deposition during a sea level rise. In contrast to other cross-shore models (e.g. Cowell et al., et al., 1999) BarSim is not constrained by the Bruun rule (Bruun, 1962) or other geometric rules (Stive and De Vriend., 1995). It has a dynamic equilibrium shoreface gradient that relates to changes in erosion and deposition at the shoreface as a function of wave characteristics and sediment supply. BarSim simulates coastal evolution in cross-section, based on rules for sediment resuspension and deposition at the shoreface, as well as backbarrier deposition (Fig. 13). Previous applications of the model have shown that BarSim is capable of reproducing the morphological evolution and stratigraphic record associated with retrogradational, aggradational and progradational wave-dominated shorelines. As the model has been described in detail in previous publications, we will restrict the discussion to the implementation of tidal deposition into BarSim.

BarSim simulates different depositional patterns for storm and fair-weather conditions. Storm conditions, defined by waves exceeding a critical height, last for short periods only, during which washover and shoreface deposition are dominant (Storms, 2003). Fair-weather conditions between successive storms, as modelled by BarSim, can last for several years. Over such long periods, tidal deposition may have

a significant influence on backbarrier deposition, for instance by decreasing backbarrier accommodation.

The rate of tidal deposition is a function of tidal amplitude, tidal prism, tidal basin area, rate of sediment supply, and sediment grain size (Van Goor et al., 2003; Chang et al., 2006). In view of the uncertainties associated with each of these factors on geological time scales, we did not attempt to simulate the full complexity of tidal deposition, but restricted ourselves to capturing its essential effects on backbarrier accommodation. In BarSim, the rate of tidal deposition is modelled as a linear function of tidal prism (tidal amplitude × basin width). In the absence of washover processes during fair weather conditions, all sediment resuspended from the shoreface by fair-weather waves is potentially available for tidal deposition. The grain-size distribution of sediments available for tidal deposition is different from the grain-size distribution of the resuspended shoreface sediment. In BarSim, it is assumed that deposition of the sand fraction is limited to the tidal channel, and tidal-flat deposits are much finer grained. Therefore, we assumed as a first estimate that 30% of the sand which is available at the shoreface will can be transported to the backbarrier area based on an evaluation of the overall simulated backbarrier fill grain-size distribution. This number will depend on local conditions, but at present no data exists to tune this variable to real-world examples of tidal deposition.

Since BarSim is a 2D model that simulates cross-shore barrier behaviour, the cross-shore profile should be interpreted as averaged over one coastal cell, thereby including both the shoreface and the tidal deltas areas. Most of the sand transported by the tidal simulation will therefore in reality end up as tidal deltas.

The upper limit on tidal deposition is determined by the backbarrier accommodation. In case the amount of sediment available for tidal deposition exceeds backbarrier accommodation, the remaining sediment will be redeposited at the shoreface. An increase in accommodation of the tidal basin under conditions of persistent sea-level rise may lead to a situation in which the increase in accommodation of the tidal basin cannot be balanced by sediment supply, which results in a gradual deepening of the tidal basin, and eventual drowning of the barrier-lagoon system (Storms and Swift, 2003; Van Goor et al., 2003). As an example of a BarSim run, Figure 14 shows the

simulated coastal response to a rising sea level across an antecedent topography that resembles the Northern Adriatic near site B. Due to the rapid increase of backbarrier accommodation, the simulated barrier cannot retrograde and is drowned. The sensitivity of this mechanism for wave-dominated and tide-dominated environments is further explained below.

6.2. BarSim simulations in tide- and wave-dominated conditions

To illustrate the generic behaviour of transgressive barrier-lagoon systems, we defined two scenarios which represent tide- and wave-dominated conditions, respectively. Both scenarios comprise 5000 years of transgression while sea level rises 20 m at a constant rate (Fig. 15). No extra sediment is added to the simulated system by longshore drift, nor is any sediment deposited by suspension fallout. In Scenario 1, the wave-dominated case, tidal amplitude is zero and transgression occurs by washover deposition exclusively. In Scenario 2, we added a macro-tidal regime (tidal amplitude = 3 m). The modelling results show that rates of transgression are comparable in both scenarios. However, it is apparent from Figure 15 that filling of the backbarrier with predominantly fine-grained sediments is, as expected, much more effective under macro-tidal conditions. The fine-grained sediments are trapped in the backbarrier, implying that erosion at the shoreface is more extensive for Scenario 2 than for Scenario 1, in accordance with the closed sediment budget in both scenarios. In Scenario 1, the depth and width of the backbarrier area increase, while the width of the barrier island decreases over time, which will eventually result in a barrier-island overstep similar to Figure 14 (Storms and Swift, 2003). A barrier-island overstep is unlikely to occur in Scenario 2. In this scenario, the width of the tidal basin also increases, but the increase in backbarrier accommodation is accompanied by an increase in the tidal prism, which in turn promotes import of sediment into the tidal basin. Hence, backbarrier deposition is much more likely to keep pace with the increasing backbarrier width.

6.3. Implications for the Adriatic barrier-lagoon systems

659 The modelling results indicate that the probability of a drowned barrier-lagoon system
660 is inversely proportional to tidal amplitude under conditions of moderate sea-level
661 rise, if all other factors are assumed equal. However, under conditions of prolonged
662 extremely rapid sea-level rise, no barrier-lagoon system is indefinitely stable (Storms
663 and Swift, 2003). Hence, under extreme conditions, it is to be expected that even tide-
664 dominated barrier-lagoon systems can be overstepped. The deep isolated sediment
665 body (Site A) appears to be a case in point. It formed during a period of significant
666 tidal amplification, as indicated by the palaeo-tidal reconstruction. According to the
667 BarSim results, this may have prevented it from being overstepped, unless sea-level
668 rise was extremely rapid. The preserved stratigraphic successions at Site A strongly
669 suggest that a barrier-island overstep did occur in the course of melt water pulse 1A.
670 Thus the inferred rate of sea-level rise during that period (~60 mm/a) would have
671 been too high for the system to maintain a dynamic equilibrium. The high rate of sea-
672 level rise also explains why the system was partially preserved, because it limited the
673 time available for wave-reworking of the drowned barrier-lagoon deposits.
674
675 The shallow isolated sediment body at Site B represents an overstepped barrier island
676 in a wave-dominated regime (Fig. 5). The rate of sea level rise at the time of overstep
677 was relatively low (~10 mm/a), but still much higher than present-day values. The
678 simulations shown in Fig. 15 illustrate transgression over a planar substrate. In case of
679 the overstepped barrier island in the Adriatic Sea, a low gradient Pleistocene plateau
680 was positioned landward of the island (Fig. 2). Backbarrier accommodation increased
681 abruptly when sea level rose above the elevation of the plateau. The presence of
682 relatively large tidal inlet-like depressions between the islands (Fig. 2) is consistent
683 with the abrupt increase in backbarrier area. The absence of significant backbarrier
684 deposits seems to indicate that tidal deposition could not compensate the abrupt
685 increase in backbarrier accommodation (Fig. 14). Barrier-island overstep at Site B
686 was therefore most likely controlled by antecedent topography.
687
688 It is not clear why the barrier-lagoon system at Site B was so well preserved, because
689 the relatively low rate of sea-level rise would have allowed sufficient time for
690 reworking of the drowned barrier-lagoon system by wave activity. A possible
691 explanation may be sought in the uncertainties surrounding our reconstructions of
692 wave climate and local rates of sea-level rise, which controlled the preservation

693 potential of the drowned barrier-lagoon system. However, other research shows
694 similar preservation potential for drowned barrier-lagoon systems (Gardner et al.,
695 2005; Gardner et al., 2007).
696
697
698 **7. Conclusions**
699
700 In our analysis of two preserved isolated sediment bodies on the Northern Adriatic
701 shelf, interpreted as barrier-lagoon systems, we combined reconstructions of
702 palaeoceanographic conditions and process-response simulations with analysis of
703 sedimentological, stratigraphic and seismic data. This multidisciplinary approach has
704 provided new insights into the formation and preservation of barrier-lagoon systems
705 during rapid sea-level rise. Our reconstructions of sea-level rise, tidal regime and
706 wave climate in the time interval between 15 ka BP and 8 ka BP indicated that the
707 conditions under which the two barrier-lagoon systems evolved were remarkably
708 different. The oldest system, present at Site A (80-90 m below present water depth),
709 formed under conditions of very rapid sea-level rise (60 mm/a), with tidal amplitude
710 of about 1.1 m, and waves that were about 15% lower than they are at present. Sea
711 level rose at about 10 mm/a during formation of the youngest system, at Site B (42 m
712 below present water depth), whereas the tidal amplitude was about the same as today
713 (~0.5 m), and wave activity was only fractionally (5%) less.
714
715 The BarSim simulations reveal that the probability of barrier-island overstepping
716 during transgression is inversely proportional to tidal amplitude, if all other factors are
717 assumed equal. Overstepping in the absence of tides is primarily caused by the fact
718 that washover is the only mechanism by which sediment can be supplied to the
719 backbarrier area. Under micro-tidal conditions, the increase in backbarrier
720 accommodation during rapid sea-level rise cannot be compensated and the backbarrier
721 deepens, leaving the barrier island isolated from the mainland. Tidal deposition
722 greatly increases the rate at which backbarrier accommodation can be filled, which
723 implies that barrier-lagoon systems under macro-tidal conditions can remain in
724 equilibrium at higher rates of sea-level rise than systems under micro tidal conditions.
725

The drowned barrier chain at Site B is separated from the palaeo-shoreline by a wide backbarrier. The presence of an overstepped barrier-island chain at the edge of a sub-horizontal plateau clearly demonstrates the overriding importance of antecedent topography on the evolution of barrier-lagoon systems. Drowning of this system appears to have been caused by the abrupt increase of backbarrier accommodation during transgression. It is not clear, however, why the system at Site B was not completely reworked, contrary to expectations based on the modest rate of sea-level rise in conjunction with the local presence of a relict sub-horizontal alluvial plain, which would imply that the overstepped barrier must have remained within reach of wave erosion for a considerable amount of time. The barrier-lagoon system at Site A does not show clear morphological evidence of overstepping. Remnants of the deep barrier system are preserved in a series of pre-existent channels dating back to a sea-level lowstand, some of which were filled with heterolithic deposits. Other channels, which appear to have formed during sea-level rise, are not filled at all. The barrier-lagoon system at Site A developed under conditions of large tidal amplitude, which permitted rapid transgression due to effective filling of backbarrier accommodation. However, this system apparently failed to keep up with the anomalously high rate of sea-level rise resulting from melt-water pulse 1A. Its preservation is thus easily explained, contrary to that of the barrier-lagoon system at Site B.

The grain-size analysis of locally preserved shoreface deposits across the Northern Adriatic shelf indicates a signature of progressive sorting related to the amount of time available for wave reworking, although the timescale associated with this phenomenon could not be established in the absence of information on the contribution of material derived from substrate erosion.

Acknowledgements

This study was carried out with financial support from the European Union (EUROSTRATAFORM research programme, contract no. EVK3-CT-2002-00079). We are grateful to Richard Signell and Klaas Scholte, for processing the bathymetric data of the Adriatic Sea, and to Albert Kettner for a preprint of his paper and providing Figure 1. ISMAR (CNR) contribution n.XXXX.

References

Amorosi, A., Colalongo, M. L., Fusco, F., Pasini, G., Fiorini, F., 1999. Glacio-eustatic Control of Continental-Shallow Marine Cyclicity from Late Quaternary Deposits of the southeastern Po Plain, Northern Italy. Quaternary Research 52,1-13.

Amorosi, A., Centineo, M.C., Colalongo, M.L., Pasini, G., Sarti, G.,Vaiani, S.C., 2003. Facies architecture and latest-Pleistocene-Holocene depositional history of the Po delta (Comacchio area), Italy. Journal of Geology 111, 39-56.

Argnani, A., Artoni, A., Ori, G.G., Roveri, M., 1991. L'avanfossa centro-Adriatica: stili strutturali e sedimentazione. St. Geol. Camerti, Vol. Spec.1, 371-381.

Artegiani, A., Bregant, D., Paschini, E., Pinardi, N., Raicich, F., Russo, A., 1997. The Adriatic Sea general circulation, part II: Baroclinic circulation structure. J. Phys. Oceanogr. 27, 1515-1532.

Bard, E., Hamelin, B., Arnold, M., Montaggioni, L., Cabioch, G., Faure, G., Rougerie, F., 1996. Deglacial sea-level record from Tahiti corals and the timing of global meltwater discharge. Nature 382, 241–244.

Belknap, D.F., Kraft, J.C., 1981. Preservation potential of transgressive coastal lithosomes on the U.S. Atlantic shelf. Marine Geology 42, 429-442.

Bondesan, M., Favero, V., Vinals, M.J., 1995. New evidence on the evolution of the Po-delta coastal plain during the Holocene. Quaternary International 29/30, 105-110.

Brunetti, A., Denèfle, M., Fontugne, M., Hatté, C., Pirazzoli, P.A., 1998. Sea-level and subsidence data from a Late Holocene backbarrier lagoon (Valle Standiana, Ravenna, Italy). Mar. Geol. 150, 29-37.

Carminati, E., Di Donato, G., 1999. Separating natural and anthropogenic vertical movements in fast subsiding areas: the Po plain (N. Italy) case. Geophys. Res. Lett. 26, 2291-2294.

Cattaneo, A. Trincardi, F., 1999. The Late-Quaternary transgressive record in the Adriatic epicontinental sea: basin widening and facies partitioning. In: Bergman, K.M., Snedden, J.W. (Eds.) Isolated Shallow Marine Sand Bodies: Sequence Stratigraphic Analysis and Sedimentologic Interpretation. SEPM Special Publication 64, 127-146.

Cattaneo, A., Correggiari, A., Taviani, M. and Trincardi, F. (2001) Sedimentologic expressions of the late-Quaternary ravinement surface in the Adriatic Sea, Italy. Int. Assoc. Sedimentol. 21th Meeting, Davos, Switzerland.

807 Cattaneo, A., Coreggiari, A. Langone, L. and Trincardi, F. (2003) The Late-Holocene
808 Gargano subaqeous delta, Adriatic shelf: Sediment pathways and supply fluctuations.
809 Marine Geology 193, 161-191.
810
811 Cattaneo, A., Steel, R.J., 2003. Transgressive deposits: an overview of their
812 variability. Earth-Science Reviews 62, 187-228.
813
814 Chang, T.S., Bartholomä, A., Flemming, B.W., 2006. Seasonal dynamics of fine-
815 grained sediments in a backbarrier tidal basin of the German Wadden Sea (Southern
816 North Sea). Journal of Coastal Research 22, 328-338.
817
818 Clark, P.U., Mitrovica, J.X., Milne, G.A., Tamisiea, M.E., 2002. Sea-Level
819 fingerprinting as a direct test for the source of global meltwater pulse IA.
820 Science 295, 2438-2441
821
822 Colantoni, P., Preti, M., Villani, B., 1990. Sistema deposizionale e linea di riva
823 olocenica sommersi in Adriatico al largo di Ravenna. Giornale di Geologia 51, 1-18.
824
825 Corps of Engineers, 1984. Shore protection manual, 4th ed. Vicksburg, Mississippi
826 Department of the Army, Waterways Experiment Station, Coastal Engineering
827 Research Center, Wahington, D.C.
828
829 Correggiari, A., Field, M., Trincardi, F., 1996a. Late Quaternary transgressive large
830 dunes on the sediment-starved Adriatic shelf. In: De Batist, M., Jacobs, P. (Eds.),
831 Geology of Siliciclastic Shelf Seas, Geological Society, London, Special Publications
832 117, pp. 155-169.
833
834 Correggiari, A., Roveri, M., Trincardi, F., 1996b. Late Pleistocene and Holocene
835 evolution of the North Adriatic sea. Il Quaternario 9, 697-704.
836
837 Cowell, P.J., Roy, P.S. Cleveringa, J. and de Boer, P.l., 1999. Simulating coastal
838 systems tracts using the shoreface translation model. In: Harbaugh, J.W., Watney,
839 W.L., Rankey, E.C., Slingerland, R., Goldstein, R.H., and Franseen, E.K. (Eds.),
840 Numerical Experiments in Stratigraphy: Recent Advances in Stratigraphic and
841 Sedimentologic Computer Simulations, Society of Economic Paleontologists and
842 Mineralogists, Special Publication 42, 371-380.
843
844 Curray, J.R., 1964. Transgression and regression. In: Miller, R.L. (Ed.). Papers in
845 Marine Geology: New York. The Macmillan Company, 175-203.
846
847 Cushman-Roisin, B., Naimie. C.E., 2002. A 3D finite-element model of the Adriatic
848 tides. Journal of Marine Systems 37, 279-297.
849
850 Decouttere, C., De Backer, K., Monbaliu, J., Berlamont, J., 1998. Wave refraction in
851 the upper Adriatic Sea. In: Gambolati G. (Ed.). CENAS. Coastline Evolution of the
852 Upper Adriatic Sea due to Sea Level Rise and Natural and Anthropogenic Land
853 Subsidence. Kluwer Academic Publishers, the Netherlands, 169-183.
854

Fairbanks, R.G., 1989. A 17,000-year glacio-eustatic sea level record - influence of glacial melting rates on the Younger Dryas event and deep-sea circulation, Nature 342, 637-642.

Fleming, K., Johnston, P., Zwartz, D., Yokoyama, Y., Lambeck, K., Chapell, J., 1998. Refining the eustatic sea level-curve since the Last Glacial Maximum using far- and intermediate-field sites. Earth and Planetary Science Letters 163, 327-342.

Forbes, D.L., Taylor, R.B., Orford, J.D., Carter, R.W.G., and Shaw, J., 1991. Gravel barrier migration and overstepping. Marine Geology 97, 305-313.

Friedman, G.M., 1961. Distinction between dune, beach and river sands from their textural characteristics. Journal of Sedimentart Petrology 31, 514-529.

Gardner, J.V., Dartnell, P., Mayer, L.A., Hughes Clarke, J.E., Calder, B.R., Duffy, G., 2005. Shelf-edge deltas and drowned barrier-island complexes on the northwest Florida outer continental shelf. Geomorphology 64, 133-166.

Gardner, J.V., Calder, B.R., Hughes Clarke, J.E., Mayer, L.A., Elston, G., Rzhanov, Y., 2007. Drowned shelf-edge deltas, barrier islands and related features along the outer continental shelf north of the head of De Soto Canyon, NE Gulf of Mexico. Geomorphology 89, 370-390.

Guillén, J., Hoekstra, P., 1996. The “equilibrium” distribution of grain size fractions and its implications for cross-shore sediment transport: a conceptual Model. Marine Geology 135, 15-33.

IDROSER, 1985. Ricerca di depositi sabbiosi sul fondo del Mare Adriatico da utilizzare per il ripascimento delle spiagge in erosione. Report Idroser S.p.A. Idrorisorse per lo sviluppo dell’Emilia-Romagna, Bologna 176 pp.

IDROSER, 1990. Ricerca di depositi sabbiosi sul fondo del Mare Adriatico da utilizzare per il ripascimento delle spiagge in erosione. 2a Campagna di ricerca. Report Idroser S.p.A. Idrorisorse per lo sviluppo dell’Emilia-Romagna, Bologna 115 pp.

Kent, D.V., Rio, D., Massari, F. Kukla, G. Lanci, L., 2002. Emergence of Venice during the Pleistocene. Quaternary Science Reviews 21, 1719-1727.

Kettner, A.J., Syvitski, J.P.M., 2007. Predicting Discharge and Sediment Flux of the Po River, Italy since the Late Glacial Maximum. IAS Special Issue (in press).

Konert, M., Vandenberghe, J., 1997. Comparison of laser grain size analysis with pipette and sieve analysis; a solution for the underestimation of the clay fraction. Sedimentology 44, 525-535.

Leatherman, S.P., 1983. Barrier island evolution in response to sea level rise: a discussion. Journal of Sedimentary Petrology 53, 1026-1031.

Liu, J.P., Milliman, J.D., 2004. Reconsidering melt-water pulses 1A and 1B: global impacts of rapid sea-level rise. Journal of Ocean University of China 3, 183-190.

Malačič, V., Viezzoli, D., Cushman Roisin, B., 2000. Tidal dynamics in the northern Adriatic Sea. Journal of Geophysical Research 105(C11), 26,265-26,280.

Malanotte-Rizzoli, P., Bergamasco, A., 1983. The dynamics of the coastal region of the northern Adriatic Sea. J. Phys. Oceanogr. 13, 1105-1130.

Nummedal, D., Swift, D.J.P., 1987. Transgressive stratigraphy at sequence-bounding unconformities: some principles derived from Holocene and Cretaceous examples. In: Nummedal, D., Pilkery, O.H., Howard, J.D. (Eds.) Sea-level fluctuation and coastal evolution. SEPM special publication 41, 241-260.

Orlic, M., Gacic, M., La Violette, P.E., 1992. The currents and circulation of the Adriatic Sea. Oceanol. Acta 15, 109-124.

Rampino, M.R., and Sanders, J.E., 1980. Holocene transgression in south-central Long Island, New York. Journal of Sedimentary Petrology 50, 1063-1080.

Rampino, M.R., and Sanders, J.E., 1982. Holocene transgression in south-central Long Island, New York-reply. Journal of Sedimentary Petrology 53, 1020-1025.

Rampino, M.R., and Sanders, J.E., 1983. Barrier island evolution in response to sea level rise: reply. Journal of Sedimentary Petrology 53, 1031-1033.

Pieri, M., Groppi, G., 1981. Subsurface geological structure of the Po plain, Italy. In:Progetto Finalizzato Geodinamica. CNR Publ. 414, 13p.

Pirazzoli, P.A., 2005. A review of possible eustatic, isostatic and tectonic contributions in eight late-Holocene relative sea-level histories from the Mediterranean area. Quaternary Science Reviews 24, 1989-2001.

Polli, S., 1960. La propagazione delle maree nell'Adriatico. Atti del Convegno dell'Associazione Geofisica Italiana, Roma 1959, 11p.

Ridente, D., Trincardi, F. (2002) Eustatic and tectonic control on deposition and lateral variability of Quaternary regressive sequences in the Adriatic basin (Italy). Marine Geology 184, 273-293.

Ridente, D., Trincardi, F., 2006. Active foreland deformation evidenced by shallow folds and faults affecting late Quaternary shelf-slope deposits (Adriatic Sea, Italy). Basin Research 18, 171–188.

Slingerland, R., Keen, T.R., 1999. Sediment transport in the western interior seaway of North America: predictions from a climate-ocean-sediment model. In: Bergman, K.M. Snedden, J.W. (Eds.) Isolated Shallow Marine Sand Bodies: Sequence Stratigraphic Analysis and Sedimentologic Interpretation. SEPM Special Publication 64, 179-190.

954 Stive, M.J.F. and De Vriend, 1995. Modelling shoreface profile evolution. Marine
955 Geology 126, 235-248.
956
957 Storms, J.E.A., 2003. Event-based stratigraphic simulation of wave-dominated
958 shallow-marine environments. Marine Geology 199, 83-100.
959
960 Storms, J.E.A., Swift, D.J.P., 2003. Shallow marine sequences as the building blocks
961 of stratigraphy: insights from numerical modelling. Basin Research 15, 287-303.
962
963 Storms, J.E.A., Weltje, G.J., Van Dijke, J.J., Geel, C.R., Kroonenberg, S.B., 2002.
964 Process-response modeling of wave-dominated coastal systems: simulating evolution
965 and stratigraphy on geological timescales. J. Sed. Res. 72, 226-239.
966
967 Swift, D.J.P., 1968. Coastal erosion and transgressive stratigraphy. Journal of
968 Geology 76, 444–456.
969
970 Swift, D.J.P., Phillips, S., Thorne, J.A., 1991. Sedimentation on continental margins,
971 IV: lithofacies and depositional systems. In: Swift. D.J.P., Oertel, G.F., R.W. Tillman,
972 R.W., Thorne, J.A. (Eds.) Shelf Sand and Sandstone Bodies. International Association
973 of Sedimentologists, Special Publication 14, 89-152.
974
975 Swift, D.J.P. and Moslow, T.F., 1982. Holocene transgression in south-central Long
976 Island, New York-discussion. Journal of Sedimentary Petrology 53, 1014-1019.
977
978 Trincardi. F., Correggiari, A., 2000. Quaternary forced regression deposits in the
979 Adriatic basin and the record of composite sea-level cycles. In: Hunt, D. Gawthorpe,
980 R.L. (Eds.) Sedimentary response to Forced Regressions. Geological Society London,
981 Special Publication 172, 245-269.
982
983 Trincardi, F., Argnani, A. (Eds.), 2001. Note Illustrative della Carta Geologica dei
984 mari italiani alla scala 1:250.000 – Foglio NL33-10 Ravenna. S.EL.CA., Firenze, 108
985 pp.
986
987 Trincardi, F., Correggiari, A., Roveri, M., 1994. Late Quaternary transgressive
988 erosion and deposition in a modern epicontinental shelf: the Adriatic Semi-enclosed
989 Basin. Geo-Marine Letters 14, 41-51.
990
991 Trincardi, F., Asioli, A., Cattaneo, A., Correggiari, A., Langone, L. 1996. Stratigraphy
992 of the late-Quaternary deposits in the Central Adriatic basin and the record of short-
993 term climatic events. In: Guilizzoni P., Oldfield F.L. (Eds.), Palaeoenvironmental
994 Analysis of Italian Crater Lake and Adriatic Sediments (PALICLAS). Mem. Ist. Ital.
995 Idrobiol. 55,39-64.
996
997 Trincardi, F., Cattaneo, A., Correggiari, A., Penitenti, D., Roveri, M., Asioli, A.,
998 Taviani, M., 2004. Geological mapping of the Italian seafloors: The Adriatic Project.
999 In: Pasquarè, G., Venturini (Eds.), Mapping Geology in Italy (APAT). S.EL.CA.,
1000 Firenze, 51-60.
1001

1002 Van Goor, M.A., Zitman, T.J., Wang, Z.B., Stive, M.J. F., 2003. Impact of sea-level
1003 rise on the morphological equilibrium state of tidal inlets. Marine Geology 202, 211-
1004 227.
1005
1006 Waschbusch, P.J., Royden, L.H., 1992. Spatial and temporal evolution of foredeep
1007 basins: lateral strength variations and inelastic yielding in continental lithosphere.
1008 Basin Research 4, 179-196.
1009
1010 Weltje, G.J., Prins, M.A., 2003. Muddled or mixed? Inferring palaeoclimate from size
1011 distributions of deep-sea clastics. Sedimentary Geology 162, 39-62.
1012
1013 Yu, S.C., Decouttere, C., Berlamont, J., 1998. Storm surge simulations in the Adriatic
1014 Sea. In: Gambolati G. (Ed.). CENAS. Coastline Evolution of the Upper Adriatic Sea
1015 due to Sea Level Rise and Natural and Anthropogenic Land Subsidence. Kluwer
1016 Academic Publishers, the Netherlands, 207-232.

FIGURE CAPTIONS

Figure 1
Overview of the study area. The greyscale shows high (dark grey) and low (light grey) lying areas. Redrawn after Kettner and Syvitski, in press.

Figure 2
(A) Overview of the Adriatic shelf with 3-D shaded bathymetry of Sites A and B. Cores used for radiocarbon dating are indicated by closed circles. Cores shown in this paper are indicated by black stars. (B) Bathymetric maps of the two sites with locations of seismic profiles.

Figure 3
Merged eustatic sea level curve (line) and associated radiocarbon datings based on Liu and Milliman (2004) and Fleming et al. (1998). Melt water pulses 1A and 1B are indicated.

Figure 4
(A) Schematic longitudinal section of the Adriatic Sea used in the 1-D palaeo-tidal reconstruction. (B) Results of the 1-D model. The left-hand side shows a series of M2 and K1 tidal amplitudes. The curves start at x=0 and extend to palaeo-coastline positions corresponding to various sea levels. On the right hand side, model results are compared to measurements of present-day M2 and K1 tides (data from Polli, 1960).

Figure 5
Reconstructed palaeo-environmental conditions on the Northern Adriatic shelf during post-glacial sea-level rise. The horizontal scale represents the coastline position during the late Quaternary transgression. (A) Maximum cumulative tidal amplitude; (B) Palaeo-wave climate; (C) Rate of sea-level change; (D) Modern bathymetry of the Adriatic shelf, with locations of the isolated sediment bodies indicated by the white areas with black stars; (E) Palaeo-coastline positions based on modern bathymetry and eustatic sea-level curve shown in Figure 3. Radiocarbon datings are from Correggiari et al., 1996a; Trincardi and Argnani, 2001, and unpublished ISMAR data (see Figure 2 for locations).

Figure 6
Shallow seismic profiles of the deep isolated sediment body at Site A. The solid white line separates the pre-transgressive (below) from the post-transgressive (above) sediment. The dotted white line in profile II highlights lateral migration structures of a channel. Profile locations indicated in Figure 2 (data from Cattaneo et al., 2001).

Figure 7
Interpreted sedimentological data of the deep isolated sediment body at Site A. For location see Figures 2 and 6 (data from Cattaneo et al., 2001).

Figure 8
Schematic cross-section of the overstepped barrier system of the shallow isolated sediment body at Site B. Vertical scale represents the water depth. Sections redrawn after Cattaneo et al. (2001).

Figure 9
Shallow seismic profiles of the low-gradient plateau at Site B. Profile VII and IX show pre-transgressive channel deposits. The arrows in profile VII indicate the direction of lateral channel migration. Profile VII illustrates the transgressive deposits. For location of the profiles see Figure 2 (data from IDROSER, 1985, 1990).

Figure 10
Grain-size data and lithofacies of seven cores taken at different water depths (see Figure 2 for locations). Vertical lines mark the occurrence of specific grain-size ranges (end members). Sucession of facies is typical for transgressive barrier-lagoon systems.

Figure 11
Mean grain size (μm) versus skewness (calculated in phi units) in all cores for three lithofacies: (A) clayey backbarrier deposits, (B) silty to sandy backbarrier deposits and (C) shoreface sands. Core locations and descriptions are shown in Figures 2 and 10. See text for explanations.

Figure 12
Mean grain size (μm) versus the rate of sea-level rise for three lithofacies: (A) clayey backbarrier deposits, (B) silty to sandy backbarrier deposits and (C) shoreface sands. Core locations and descriptions are shown in Figures 2 and 10. See text for explanations.

Figure 13
Basic concepts of the numerical model BarSim (Storms et al., 2002; Storms, 2003).

Figure 14
Example of a BarSim run for a situation comparable to the coastal evolution history at site B. The upper panel shows that initially no barrier was present at the steep part of the edge of the plateau. As the barrier formed and migrated landward (panel 2-4) the depth and width of the backbarrier rapidly increased which led to overstepping (panel 5).

Figure 15
BarSim simulations for a transgressive wave-dominated (Scenario 1) and tide-dominated (Scenario 2) barrier-lagoon system. Simulated time interval = 5000 years; relative sea-level rise = 20 m. Tidal amplitude in Scenario 2 = 3 m. Gray-scale represents mean grain size (dark = coarse, light = fine). Synthetic cores at final coastline positions are shown on the right. (C) Super-imposed final morphologies of the two systems.

1109 Figure 1
1110

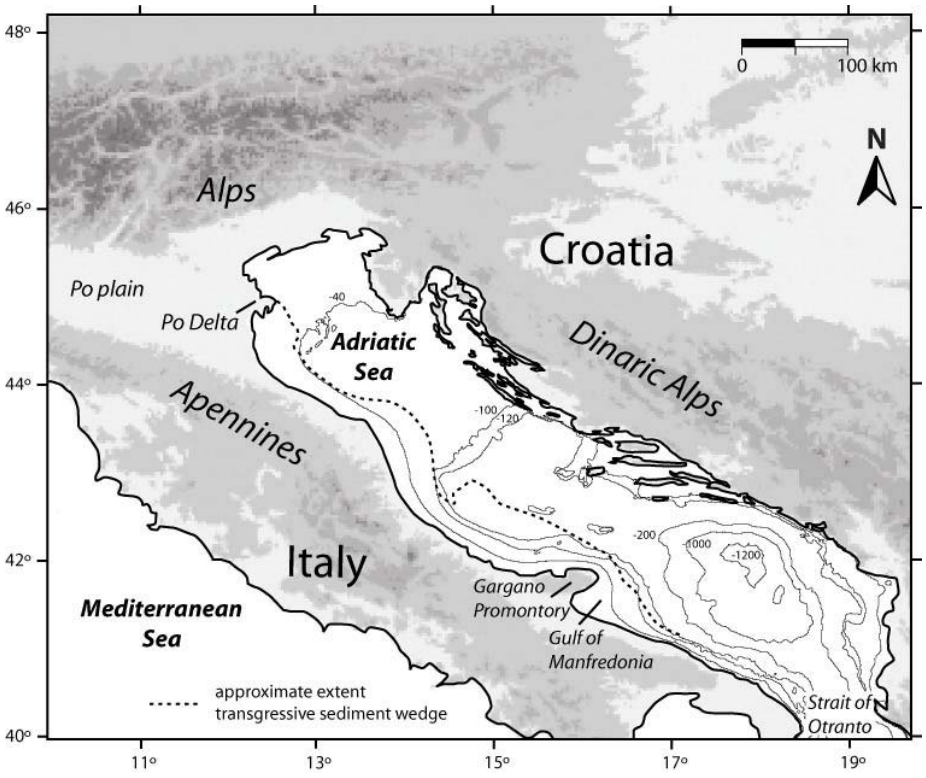

1111

1112 Figure 2

1113

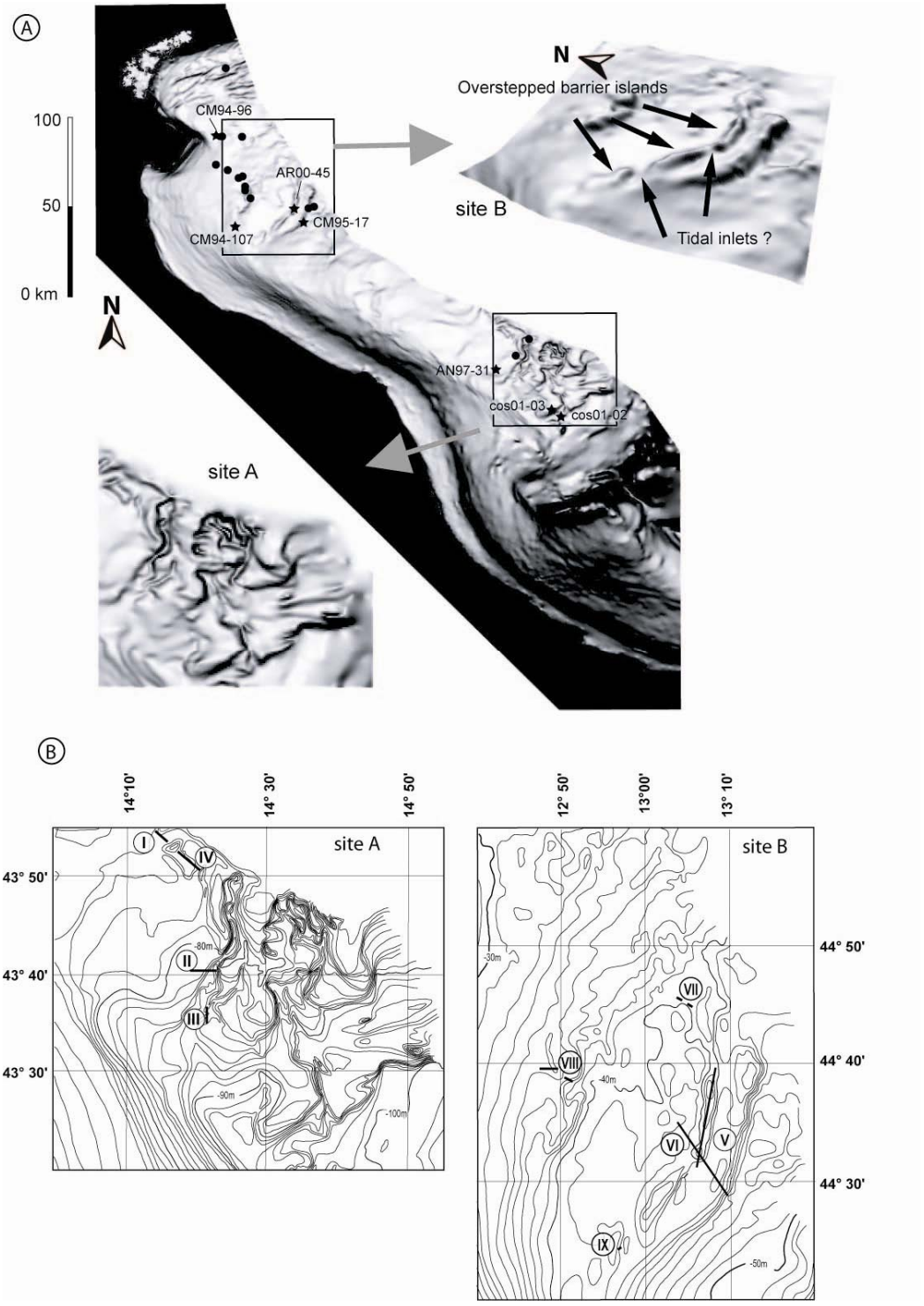

1114

1115 Figure 3

1116

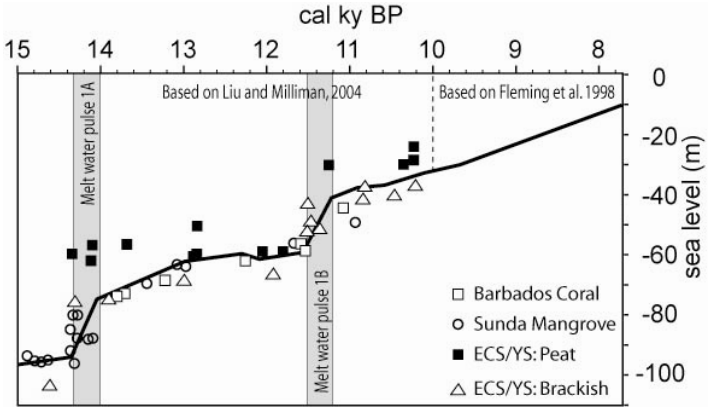

1117

1118 Figure 4
1119

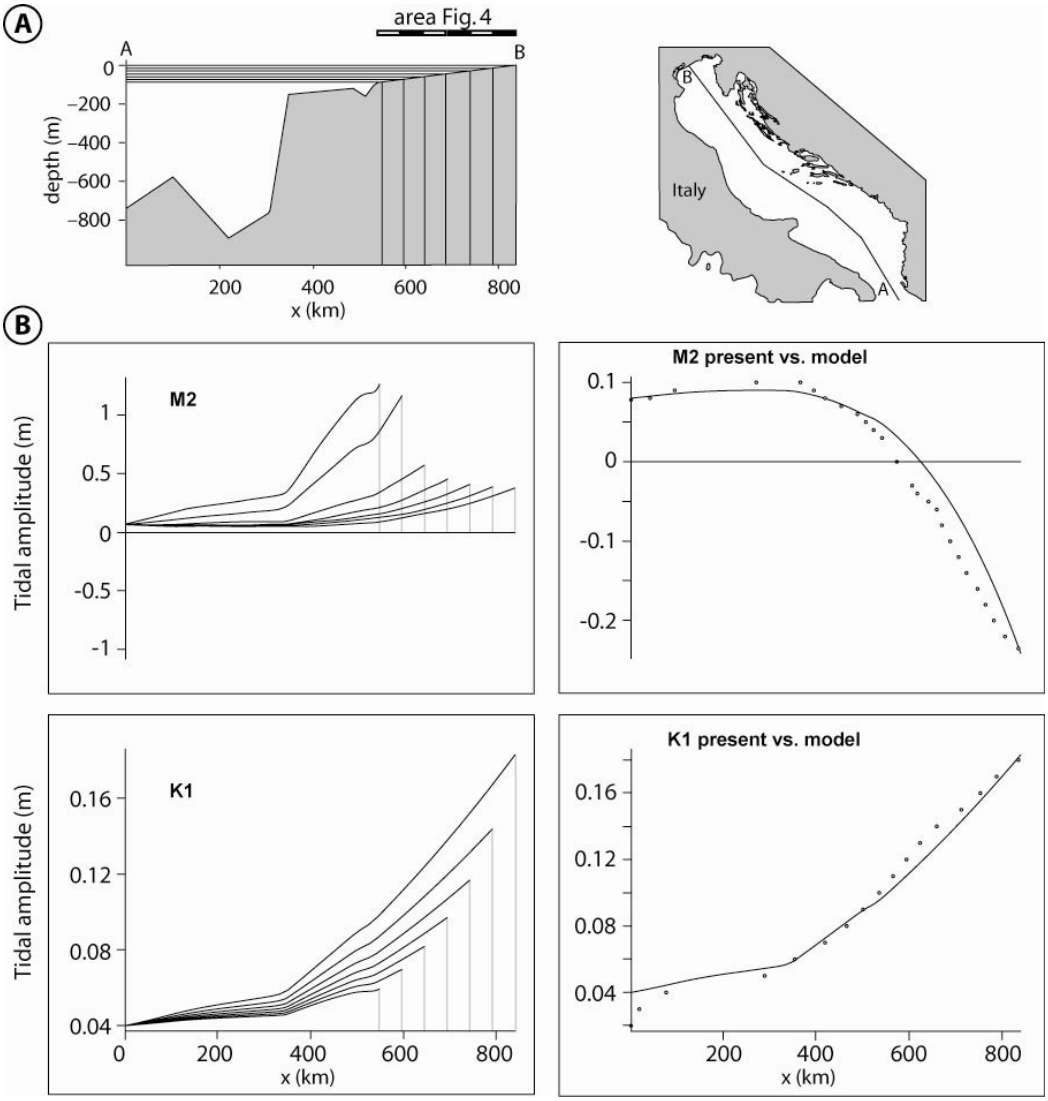

1120

1121 Figure 5

1122

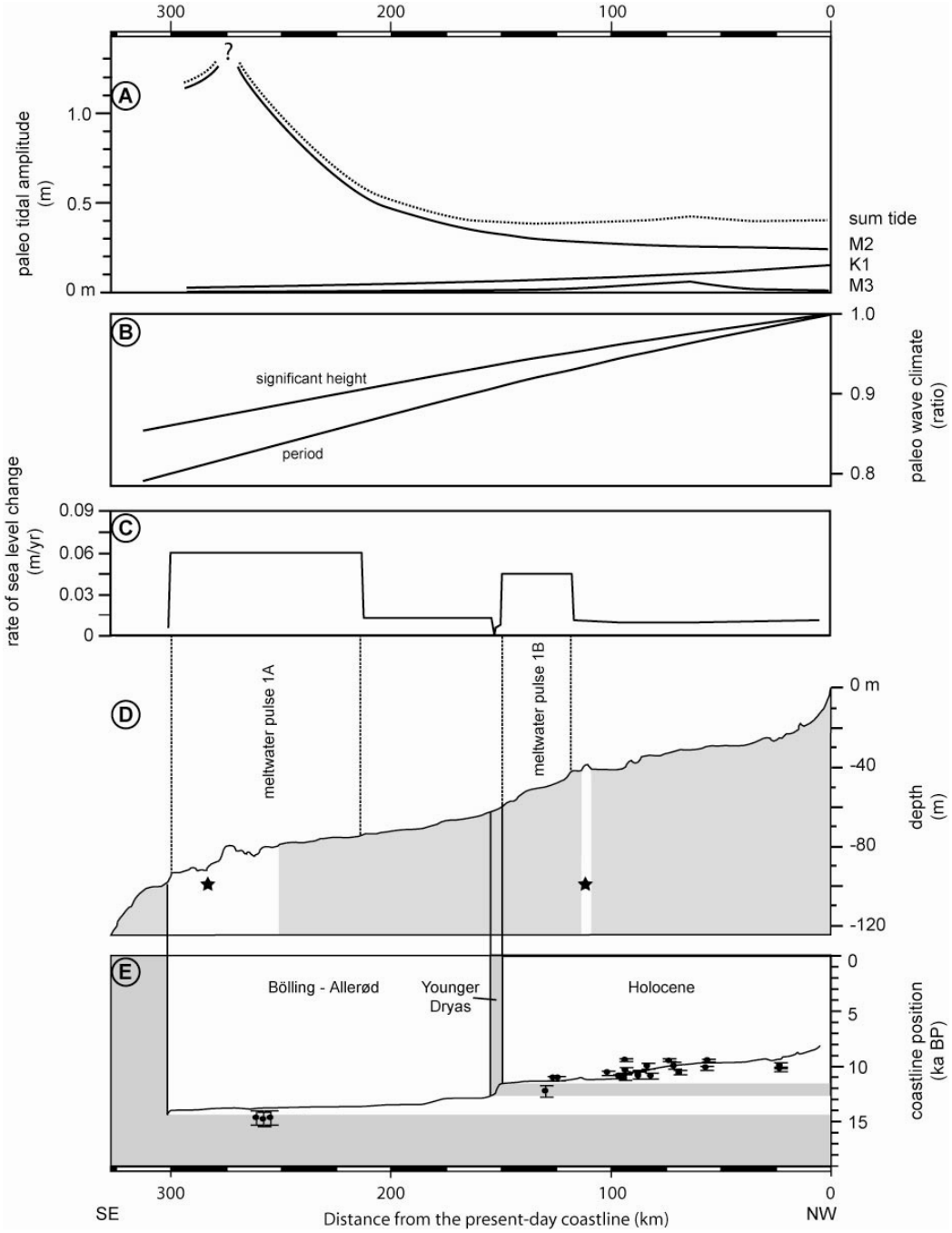

1123

1124 Figure 6

1125

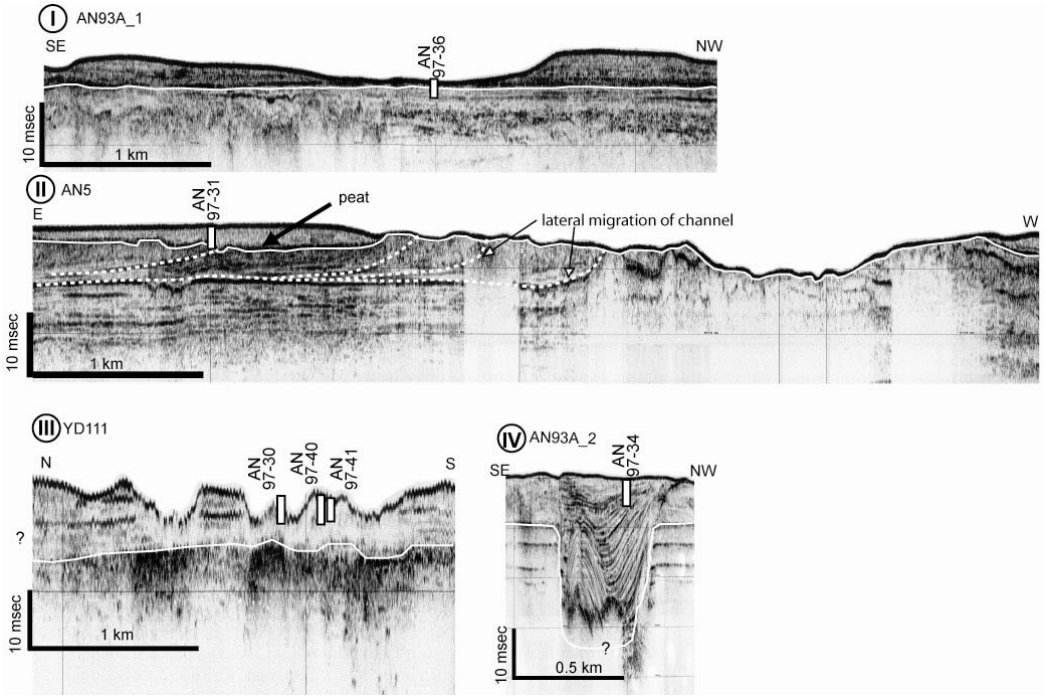

1126

Figure 7

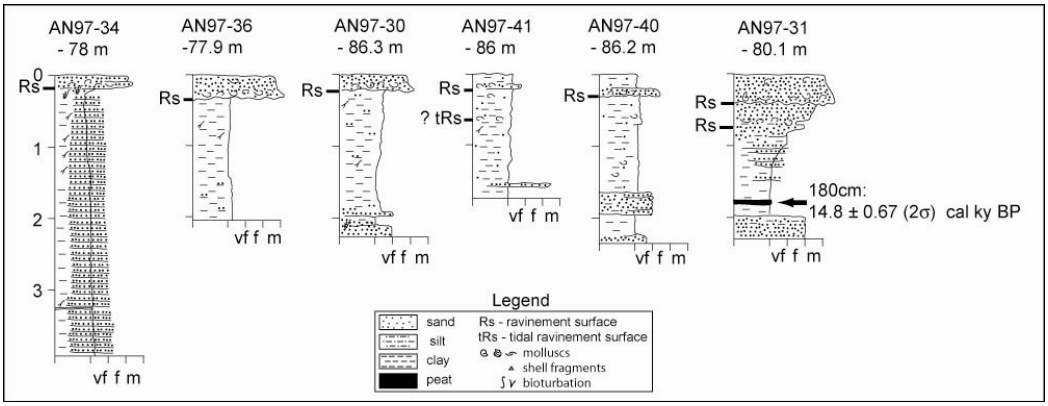
AN97-34
- 78 m
AN97-36
-77.9 m
AN97-30
- 86.3 m
AN97-41
- 86 m
AN97-40
- 86.2 m
AN97-31
- 80.1 m
0
1
2
3
Rs
? tRs
vf f m
180cm:
14.8 ± 0.67 (2σ) cal ky BP
Legend
sand
silt
clay
peat
Rs - ravinement surface
tRs - tidal ravinement surface
molluscs
shell fragments
bioturbation

1131 Figure 8

1132

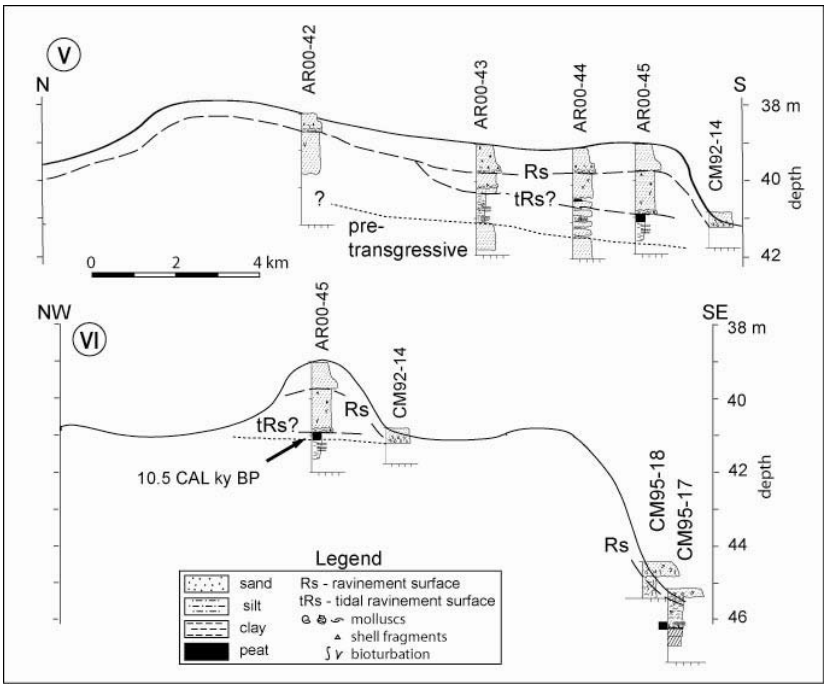

1133

1134 Figure 9

1135

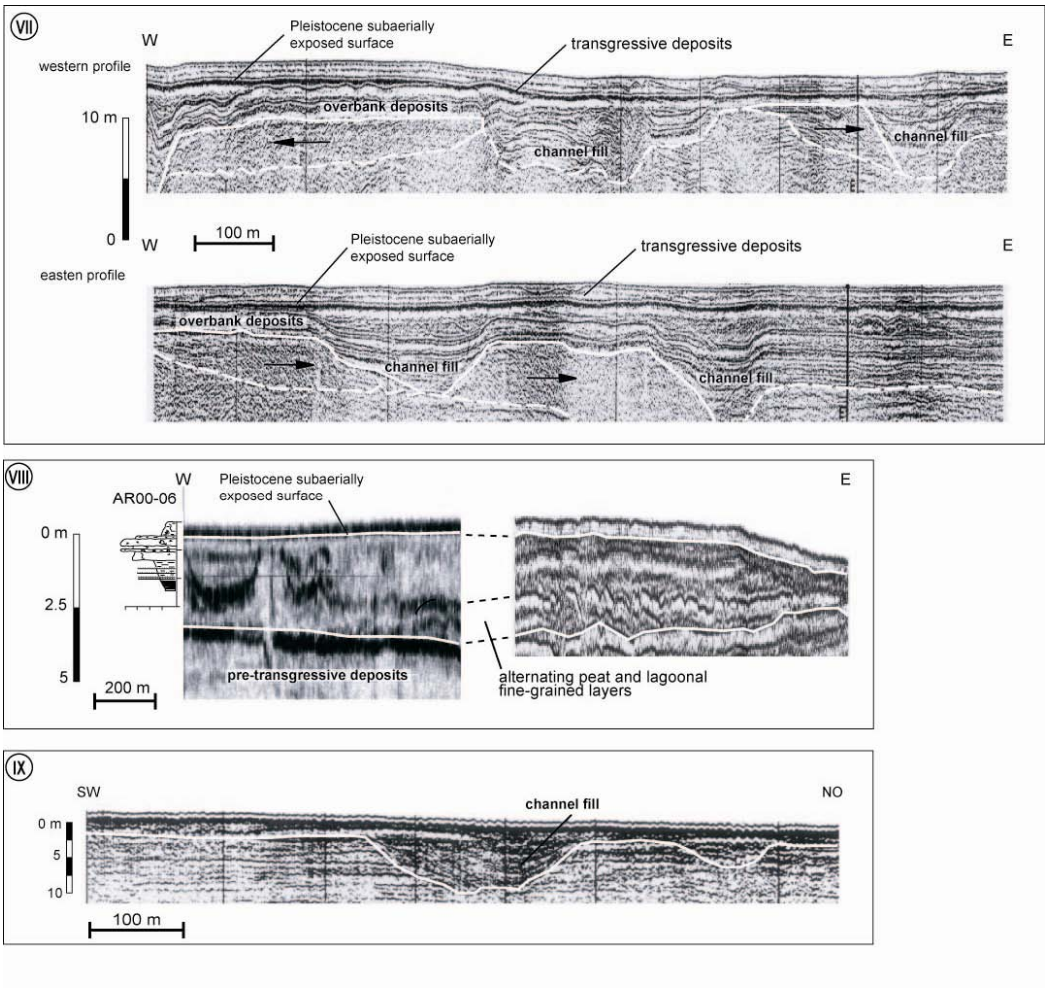

1136

1137 Figure 10

1138

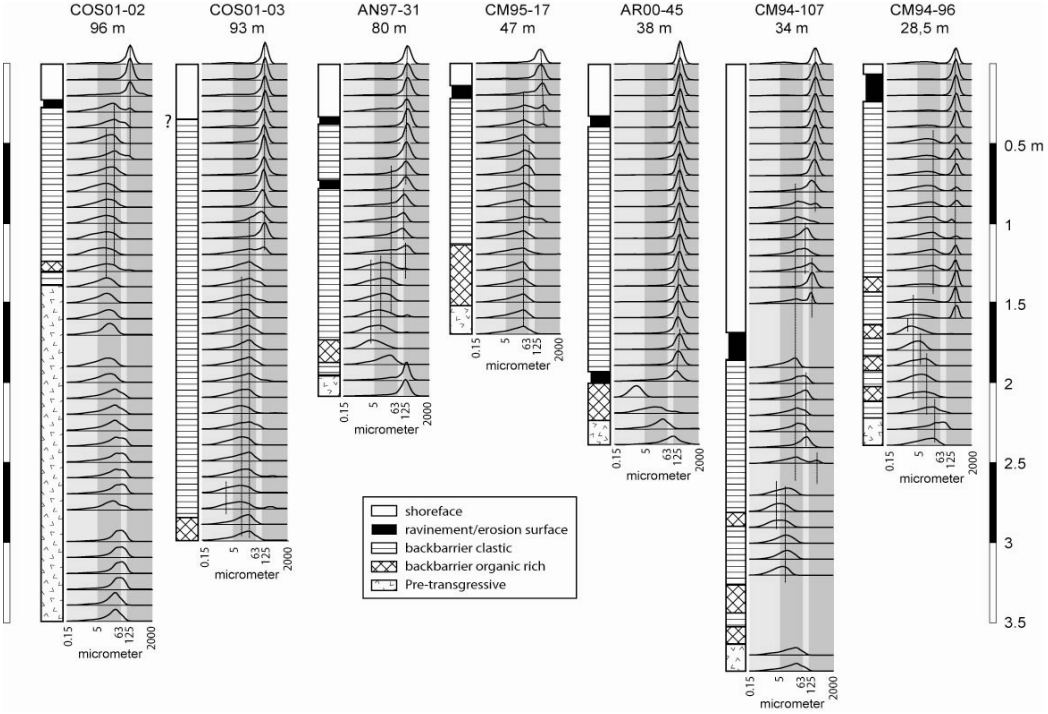

1139

1140 Figure 11
1141

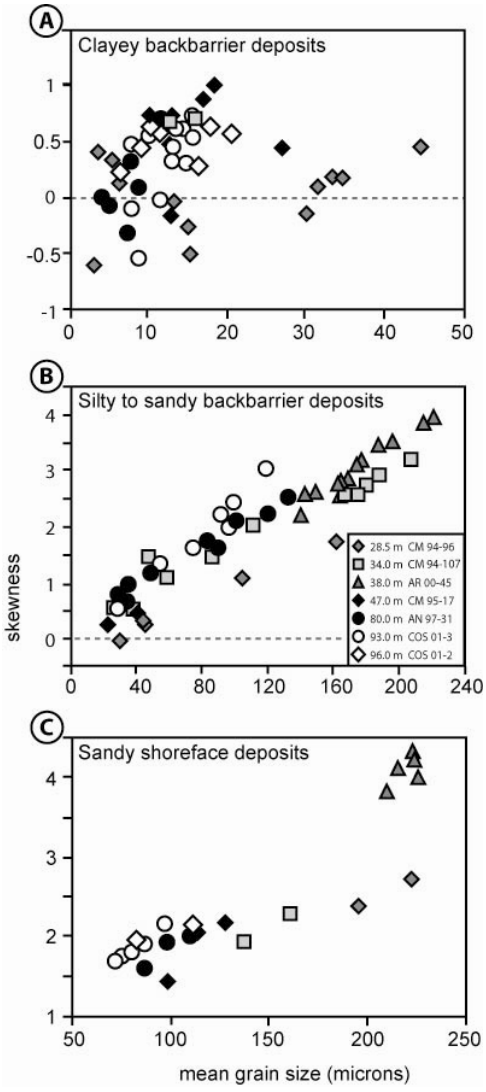

1142

1143 Figure 12

1144

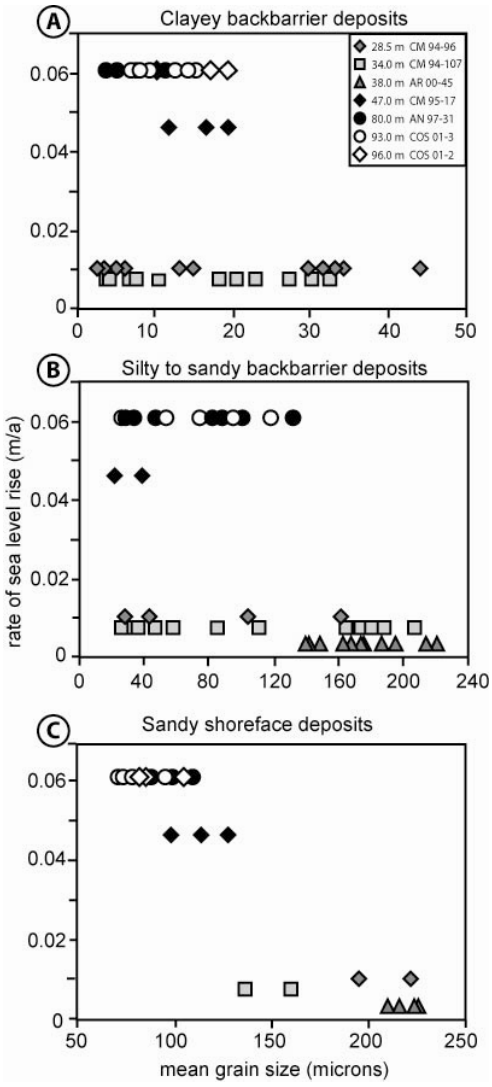

1145

1146 Figure 13
1147

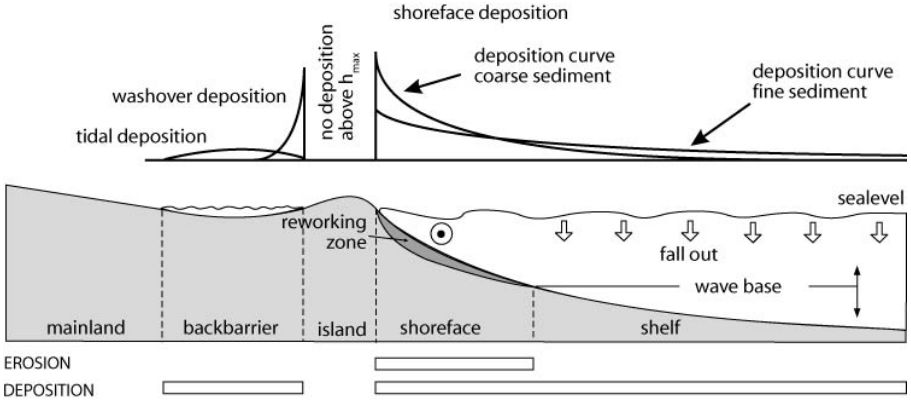

1148

1149 Figure 14
1150

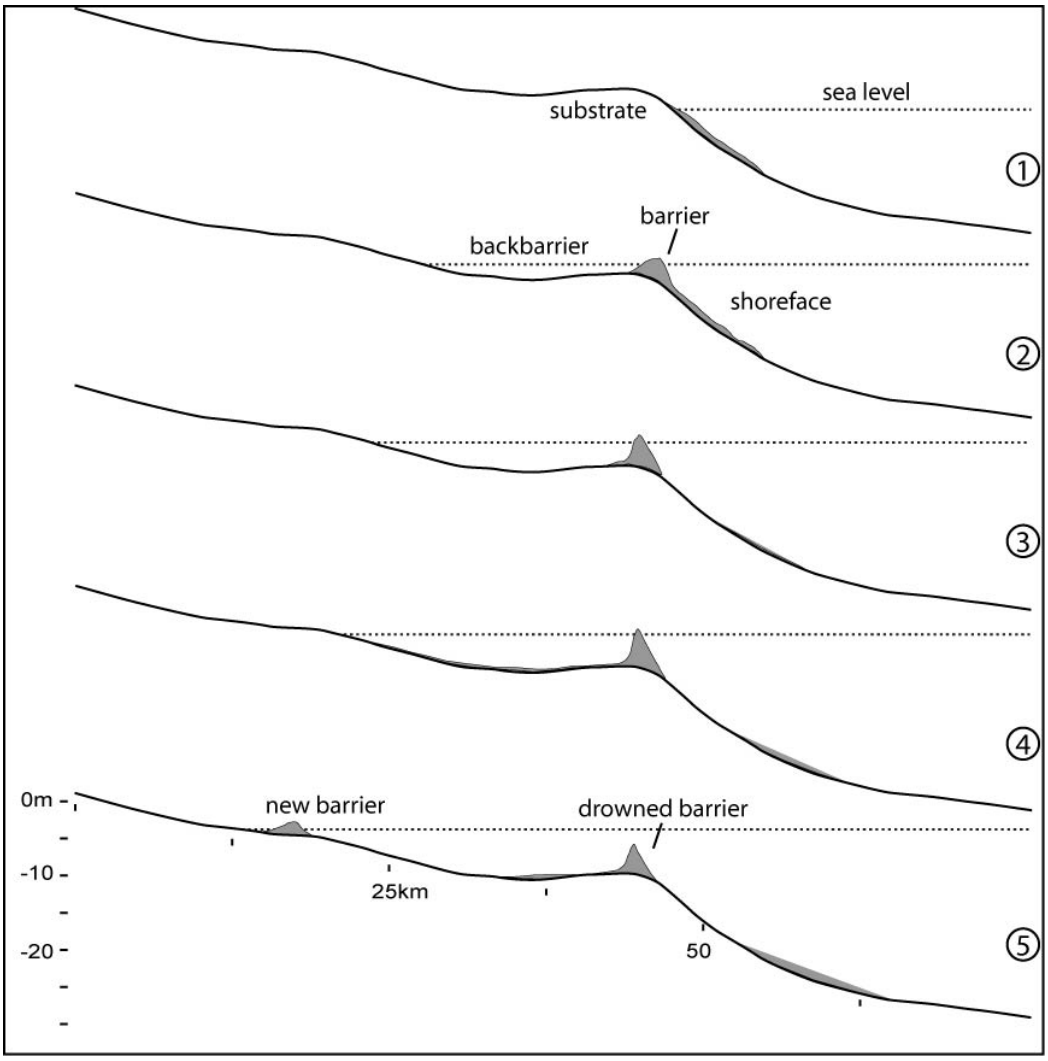

1151

1152 Figure 15

1153

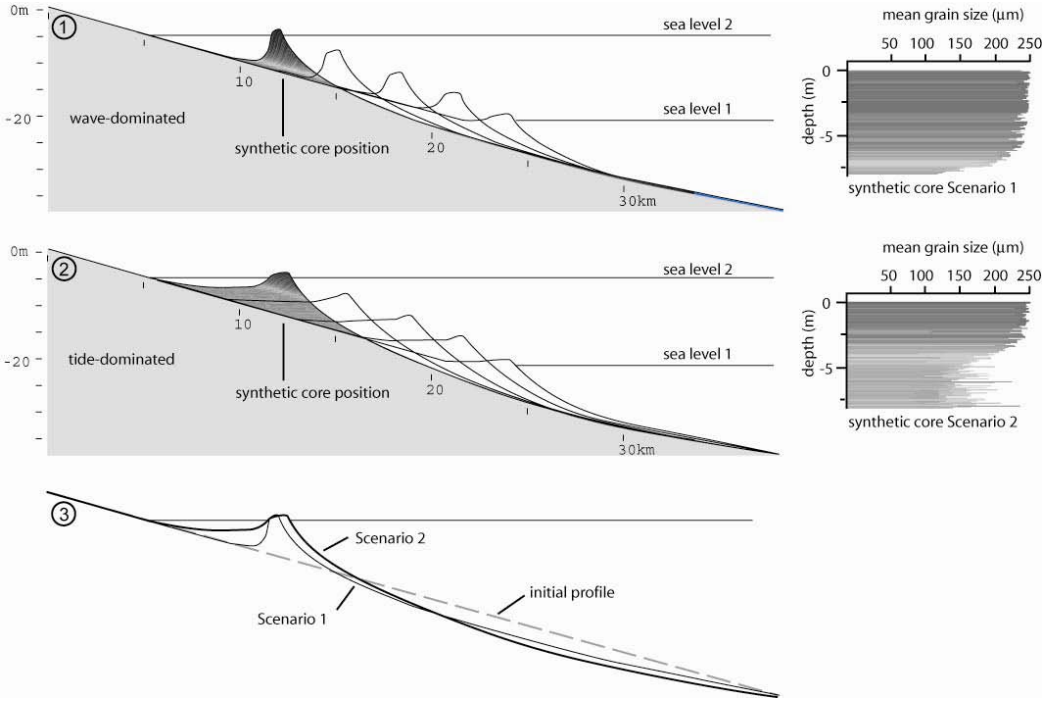

1154